Supplemental Methods

I. Post-mortem brain samples

Postmortem brain tissue was obtained from the Douglas-Bell Canada Brain Bank (www.douglasbrainbank.ca). This facility collects brains from subjects who died by suicide as well as from psychiatrically healthy control subjects. Once a family accepts to make a donation, a series of interviews known as psychological autopsies (1) are carried out, whereby information is obtained by means of structured interviews on psychiatric history (Axis I and Axis II), psychological traits, development, life events and history of trauma/abuse. These lengthy interviews are then complemented by information from medical charts, police and coroner records. In addition, extensive demographic and medical information is collected which includes history of medical treatment (2, 3). Psychological autopsies were performed post-mortem on both cases and controls by a panel of psychiatrists and diagnoses were assigned based on DSM-IV criteria. The control group was composed of individuals who died suddenly from accidental causes or myocardial infarction, and could not have undergone any resuscitation procedures or other type of medical intervention. Controls had no history of psychopathology, including suicidal behavior or major mood or psychotic disorders (**Supplementary Table 1**). Brains were rapidly preserved upon arriving at the Brain Bank, and the left hemisphere was cut into consecutive 1 cm-thick coronal sections that were snap-frozen and stored at -80˚C. Dissections from thick frozen sections were performed on dry ice, following well-established anatomic landmarks. Specifically, grey matter was dissected from the dACC, adjacent to the dorsal part of the genu of the corpus callosum (BA24) (4, 5). The anterior region immediately dorsal to the genu of the corpus callosum was located as shown by Hersher *et al.* in Figure 1 (6) and 1-cm^3 tissue blocks were removed while maintaining the tissue on dry ice until RNA extraction was performed. Cases in this study were individuals who had a diagnosis of BD type I or type II (N = 13). Controls (N = 13) had neither current nor past psychiatric diagnoses. Cases and controls were matched for refrigeration delay, age, brain pH, and RNA integrity number, and there were no group differences in these variables. Refrigeration delay refers to the difference between the estimated time of death (determined by the pathologist through external body examination details) and the time at which the brain was refrigerated.

II. High throughput transcriptome sequencing

Total RNA was extracted from brain tissue sections using the RNeasy system (Qiagen). RNA quality and concentrations were measured on a Nanodrop 2000 Spectrophotometer and an Agilent 2100 Bioanalyzer. In order to maintain the long non-coding RNA fraction that does not contain a polyA-tail, we selected RNA for sequencing using ribosomal depletion. A starting amount of 4ug total RNA was used according to the RiboZero (Epicentre) protocol for ribosomal depletion. Briefly, the total RNA was incubated with ribosomal (rRNA) sequence-specific 5'-biotin labeled oligonucleotide probes. Following probe hybridization, the rRNA/probe complex was removed from the sample with streptavidin-coated magnetic beads, leaving behind only 10-20% of the total RNA fraction. This fraction was used to create RNAseq libraries following the TruSeq dUTP degradation-based directional protocol (Illumina). All sequencing for this project was carried out at the Genome Quebec Innovation Center

using the Illumina HiSeq 2000 platform. In order to achieve adequate coverage of the transcriptome including lowly expressed transcript variants, one library was sequenced per lane (**Supplementary Table 2**). Throughout the library preparation a randomization process was used to ensure that no batch effects were generated. Briefly, we identified four batching stages each with different samples per batch: ribosomal depletion (n=6), library preparation (n=8) and sequencing flow cell (n=8). We randomized the samples in each batch and then tested correlations with possible confounders: Diagnosis, pH Value, Post-mortem Delay, Gender, Age, Cause of Death and RIN. This ensured that there would be no batch effects going into the experiment.

III. Bioinformatics analyses

Alignment. Following high-throughput sequencing, 100bp paired-end reads were aligned to the human genome reference (hg19) using TopHat v2.0.8b (http://tophat.cbcb.umd.edu/)(7) with a mate insert distance of 75 bp (-r) and library type fr-firststrand. Those reads that passed mapping quality of at least 50 were used for gene and transcript quantification.

Quantification. Gene annotations were assembled by combining the annotations from the Illumina iGenomes UCSC (hg19) which corresponds to Ensembl annotations downloaded on March 6, 2013 (Ensembl release 70) (https://support.illumina.com/sequencing/sequencing_software/igenome.ilmn). SmallRNA annotation files were downloaded from miRBase release 19. Additional lincRNA annotations were obtained from the lincRNA catalog stringent set downloaded on Sep 20 2013 (http://www.broadinstitute.org/genome_bio/human_lincrnas/sites/default/files/lincRNA_catalog/lincRNAs_transcripts_stringentSet.gtf)(8).

For gene-level quantification we used HTSeq-count version 0.5.4p1 (http://www-huber.embl.de/users/anders/HTSeq/doc/overview.html) to count fragments that overlap genes identified through the annotations described(9). HTSeq-count was ran with the intersection-nonempty mode and reverse strand parameters for each sample and the results were combined to form a count matrix of 60,905 transcribed RNAs across 26 samples (**Supplementary Figure 1)**. As validation, we also ran Cufflinks v2.1.1 (http://cufflinks.cbcb.umd.edu/)(10) to count fragments at the gene as well as transcript level using the same gene annotation files as for HTSeq-count with parameters --multi-read-correct and --library-type fr-firststrand for each sample and the results were combined to form a FPKM matrix of 60,327 transcribed RNAs across 26 samples (**Supplementary Figure 1)**. Due to differences between the tools' counting algorithms, the FPKM matrix was approximated to a count matrix where gene lengths were obtained by summing the exon length for each gene using the hg19 ensGene table in the GenomicFeatures_1.12.2 R package (http://www.bioconductor.org/packages/release/bioc/html/ GenomicFeatures.html). The library size for each sample was estimated using the number of mapped reads in the BAM file using 'samtools view -c' (http://samtools.sourceforge.net/) command.

Differential expression analysis. All whole-transcript and isoform matrices were analyzed separately. For each transcript, we summed the mapped fragments across all samples. We removed those transcripts with no mapped fragments. In addition, those transcripts whose total is

greater than 34.7 million mapped fragments (or 1% of the total for all the transcripts) were also removed. Fragments were normalized across libraries by using the weighted trimmed mean of log expression ratios (TMM) from the edgeR v3.0.8 R package (11). Furthermore, genes and isoforms with low counts were removed by keeping only those which have counts of at least 0.2 CPM (counts per million) in at least 8 samples per group. Counts were corrected for heteroscedasticity by employing voom from the limma v3.14.4 R package (12). The linear model used to fit the data included diagnosis, postmortem interval (PMI) and RNA integrity number (RIN) as covariates. Gene annotations were incorporated using the biomaRt v2.14.0 R package (http://www.bioconductor.org/packages/release/bioc/html/biomaRt.html).

External validation cohort analysis. We obtained RNAseq data (13) from the Stanley Neuropathology Consortium Integrative Database (SNCID) Array Collection consisting of 61 thoroughly characterized samples (BD=26, CTRL=35) from the anterior cingulate cortex described previously (14). Fragments were aligned to the human (hg19) reference genome using STAR_2.4.0h (15) fragments were mapped to genes using featureCounts from the subread-1.4.6 package (16, 17) with a minimum quality of 50. Ensembl gene annotations were obtained from the Illumina iGenomes UCSC (hg19) (Ensembl release 70, March/6/2013) (https://support.illumina.com/sequencing/sequencing_software/igenome.ilmn). Gene expression levels were normalized using the TMM method followed by employing voom from the limma v3.14.4 R package (12).

Comparison to dorsolateral prefrontal cortex (DLPFC) external dataset. In order to compare our results with those of one previous transcriptome sequencing study in BD (18), raw count expression matrices deposited by Akula *et al.* were obtained from the Gene Expression Omnibus (GEO, GSE53239). Expression matrices from the two platforms described by *Akula et al*. (NISC1 and NISC2) were combined and batch-corrected by removing the first principal component. The first principal component contributed to the 20% of the variance and the scores were significantly different between the two platforms ($P < 0.001$, t-test). The list of differentially expressed transcripts was identified by applying the same procedure used for our data. We performed an over-representation analysis by compiling the list of downregulated transcripts ($p<0.01$) from one study and calculating the AUC against the entire list of downregulated transcript p-values from the other study. We repeated this analysis for upregulated transcripts. ROC curves were plotted with the pROC_1.7.2 R package (19).

IV. Neural Progenitor Cell lines chronic drug treatment experiments

Cell culture and treatments. Human neural progenitor cells (NPCs) derived from induced pluripotent stem cell (iPSC) line GM08330 obtained from a healthy male and previously characterized (20), were generously provided by Dr. Stephen Haggarty. NPCs were maintained on culture plates coated with 200µg/ml Poly-L-ornithine hydrobromide (Sigma) and 5mg/ml laminin (Sigma) and maintained in media with 70% DMEM (Invitrogen), 30% Ham's F12 (Mediatech), 1x penicillin/streptomycin (Invitrogen) and supplemented with B-27 (Invitrogen). During expansion cells were grown in media containing 20ng/ml of human EGF (Sigma), FGF (R&D Systems) and 5µg/ml heparin (Sigma). To induce neural differentiation, cells were allowed to reach 90% confluence before growth factors were removed. At this point chronic (1 week) treatments were performed with drugs commonly prescribed in bipolar disorder: lithium, valproic acid, and carbamazepine. To find adequate drug concentrations

for treatment, cells were screened for cytotoxic effects by measuring the activity of mitochondrial dehydrogenase using the 3-(4, 5-dimethylthiazol-2-yl)-2, 5-diphenyltetrazolium bromide (MTT) assay (Sigma-Aldrich Co) with three different concentrations tested for each drug in accordance with the literature and estimates of the correspondence to clinical treatment levels in patients. For lithium, concentrations of 0.5M, 1.0M, and 2.0M were tested. For valproic acid, concentrations of 0.5M, 1.0M, and 2.0M were tested. For carbamazepine, concentrations of 25mM, 50mM, and 100mM were tested. No significant toxicity was detected at any concentration, thus, cells were treated with 1.0 mM lithium chloride (Li), 1.0 mM valproic acid (VPA), 50uM carbamazepine (CBZ), or no-drug control for one week, after which cell pellets were collected and RNA was extracted. All experiments were performed in triplicate.

Immunohistochemistry. In order to validate the neuronal and astroglial properties of neural progenitor cell lines, we performed immunohistochemistry with neuron-specific and astrocyte-specific markers MAP2 and GFAP respectively. Cover slips were washed 3 times for 5 minutes in TBS + 0.05% tween and incubated for 20 minutes in a solution of 1% bovine serum albumin (BSA) and 0.2% Triton in PBS. This was followed by an hour pre-incubation in a solution of 1% BSA in PBS containing 5% Normal goat serum (NGS) before being transferred one hour in the same solution containing anti- Map2 (1:1, 0000, Abcam, Cambridge, MA, USA) and GFAP (1:1000, Dako, Burlington, ON, CA)) antibodies for two hours. Cover slips were then incubated 2h with secondary goat anti-rabbit antibody coupled to Texas red (1:1000, Abcam, Cambridge, MA, USA) and a donkey anti-mouse antibody coupled with the florophore FITC (1:1000, Vector Laboratories Inc., Burlington, ON, Canada). Sections were mounted on glass slides, and coverslipped with Prolong gold with Dapi (Fisher Scientific Inc., Pittsburgh, PA, USA).

V. Quantitative Real-time Polymerase Chain Reaction (qRT-PCR)

Total RNA was extracted from frozen brain tissue using the RNeasy Lipid Tissue Mini Kit (Qiagen) and from frozen cell pellets using the RNeasy Mini Kit (Qiagen). Brain RNA for validation of RNASeq results was from the same original extraction. Synthesis of cDNA was performed in triplicated, using M-MLV reverse transcriptase (Gibco, Burlington, Ontario) along with oligo(dT)16 primers (Invitrogen) and random hexamers (IDT DNA) in a 1:1 ratio. Real-time PCR reactions were run in quadruplicate using an ABI PRISM 7900HT Sequence Detection System (Applied Biosystems) and the iTaq Universal SYBR Green Supermix (BioRad). Extensive characterization of all SYBR Green assays was undertaken to ensure single-product specificity and efficiency compatibility with endogenous controls (Data not shown). All primer sequences and reaction parameters are available upon request. Relative expression was calculated using the relative quantitation method (ΔΔCt) in the RQ Manager 1.2 software (Applied Biosystems). We investigated the stability of various endogenous genes prior to performing qRT-PCR experiments in each sample set and determined the most suitable endogenous gene using the NormFinder Algorithm (21) (**Supplemental Table 3**). All qRT-PCR experiments were reported with POLR2A (Polymerase (RNA) II (DNA directed) polypeptide A) or ACTB (Beta Actin) as endogenous control.

Supplemental Figures

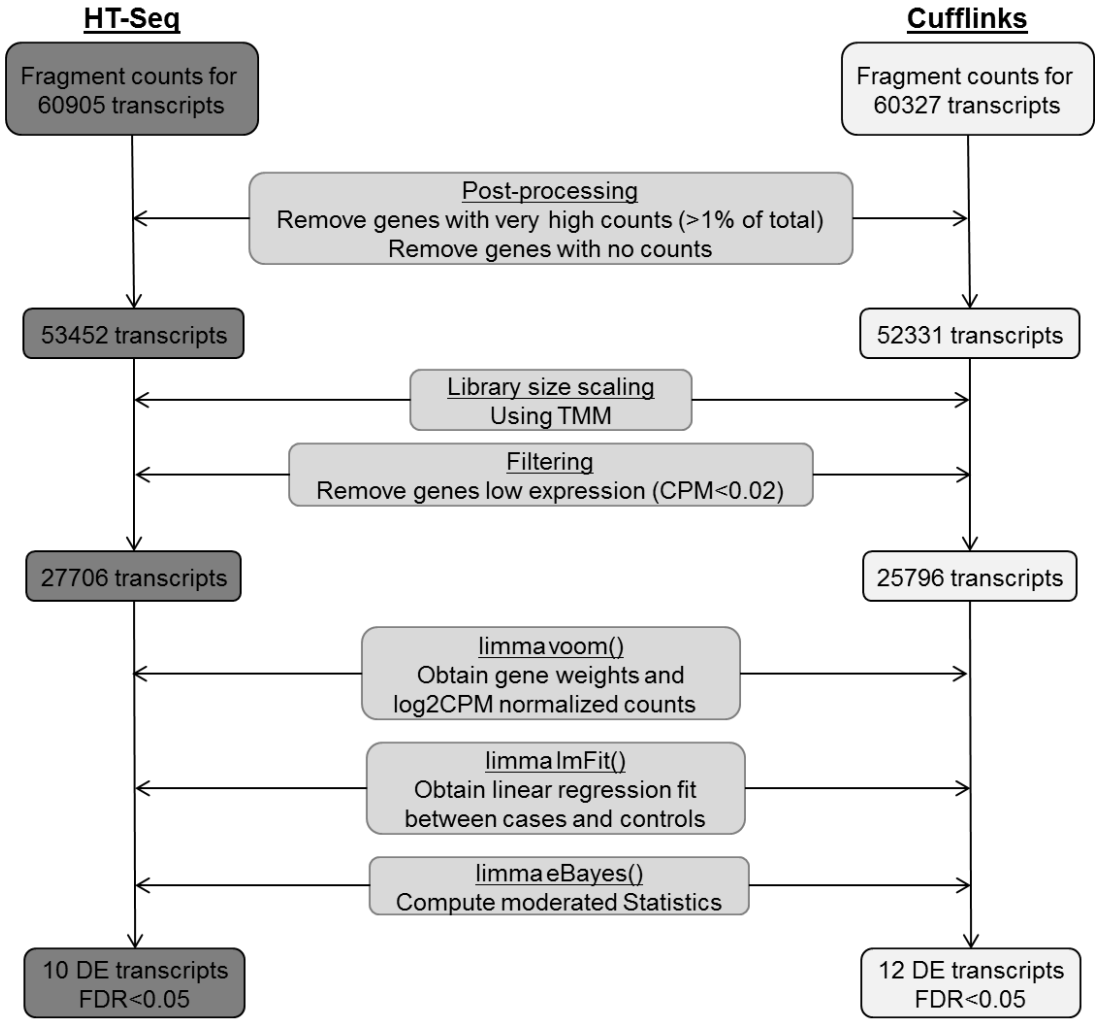

Figure S1: Gene-level differential expression bioinformatics analyses – consistency between two methods.

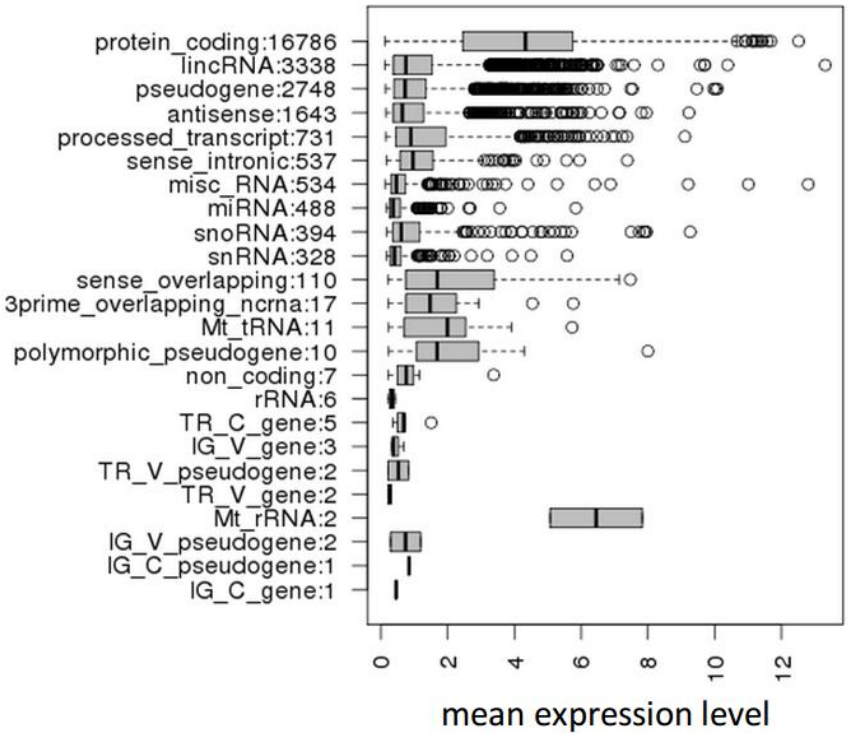

Figure S2: Mean expression statistics for the different RNA classes after filtering. The numbers after each RNA class indicate the number of genes that belong to that class.

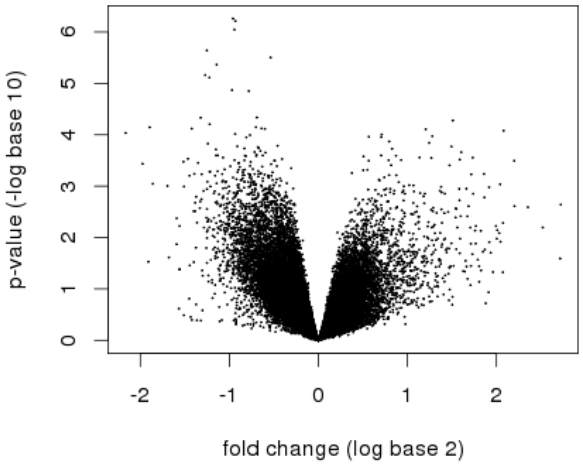

Figure S3A: Volcano plot that shows the overall transcript differential expression for all genes from the HT-Seq analysis. There is a stronger effect for downregulated (negative fold change) as opposed to upregulated genes (positive fold change).

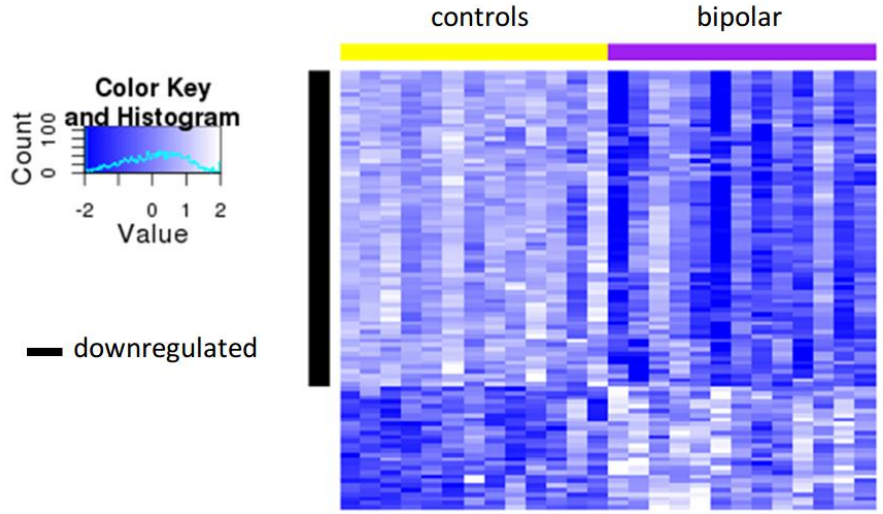

Figure S3B: Hierarchical clustering of the top 100 transcripts (ranked by increasing p-value) across controls and bipolar samples, 72 of which are downregulated. Expression levels have been mean centered and normalized.

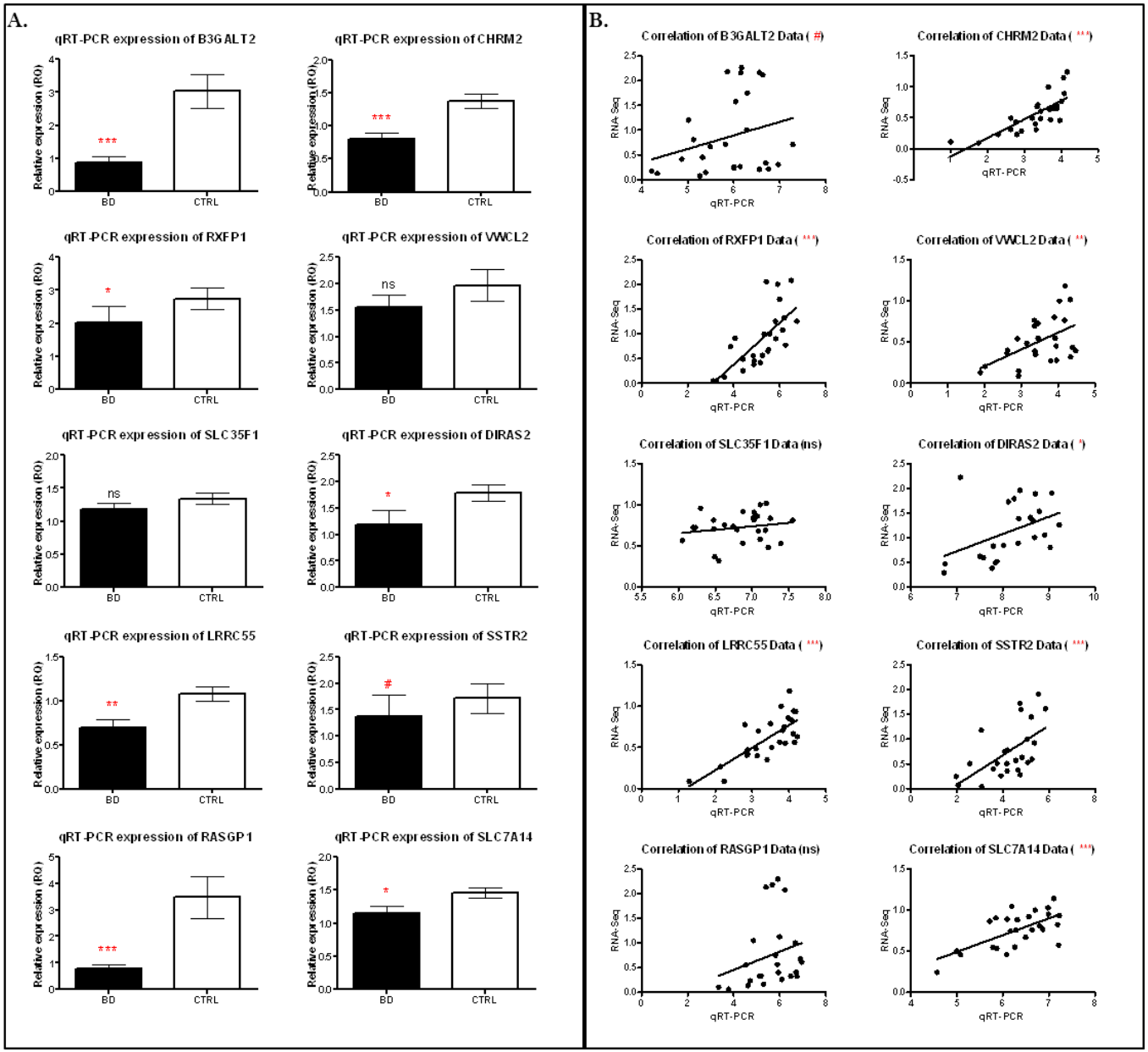
A.
qRT-PCR expression of B3GALT2
Relative expression (RQ)
***
BD
CTRL
qRT-PCR expression of CHRM2
Relative expression (RQ)
***
BD
CTRL
qRT-PCR expression of RXFP1
Relative expression (RQ)
*
BD
CTRL
qRT-PCR expression of VWCL2
Relative expression (RQ)
ns
BD
CTRL
qRT-PCR expression of SLC35F1
Relative expression (RQ)
ns
BD
CTRL
qRT-PCR expression of DIRAS2
Relative expression (RQ)
*
BD
CTRL
qRT-PCR expression of LRRC55
Relative expression (RQ)
**
BD
CTRL
qRT-PCR expression of SSTR2
Relative expression (RQ)
#
BD
CTRL
qRT-PCR expression of RASGP1
Relative expression (RQ)
***
BD
CTRL
qRT-PCR expression of SLC7A14
Relative expression (RQ)
*
BD
CTRL
B.
Correlation of B3GALT2 Data (#)
RNA-Seq
qRT-PCR
Correlation of CHRM2 Data (***)
RNA-Seq
qRT-PCR
Correlation of RXFP1 Data (***)
RNA-Seq
qRT-PCR
Correlation of VWCL2 Data (**)
RNA-Seq
qRT-PCR
Correlation of SLC35F1 Data (ns)
RNA-Seq
qRT-PCR
Correlation of DIRAS2 Data (*)
RNA-Seq
qRT-PCR
Correlation of LRRC55 Data (***)
RNA-Seq
qRT-PCR
Correlation of SSTR2 Data (***)
RNA-Seq
qRT-PCR
Correlation of RASGP1 Data (ns)
RNA-Seq
qRT-PCR
Correlation of SLC7A14 Data (***)
RNA-Seq
qRT-PCR

Figure S4: A: qRT-PCR results in BA24. **B**: Correlations between RNASeq and qRT-PCR expression values.

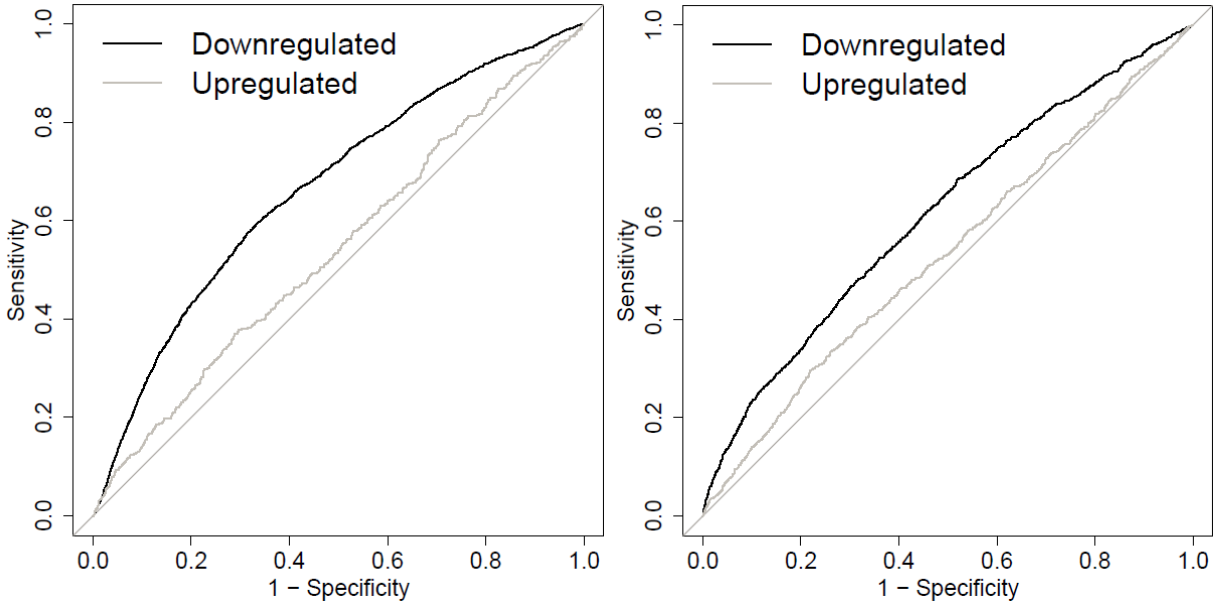

Figure S5: A. Left, Downregulated transcripts tended to be downregulated in a separate study. Top downregulated transcripts (p-value < 0.01) are overrepresented among the top downregulated transcripts in Akula *et al.* **B. Right**, Top downregulated transcripts from Akula et al. (p-value < 0.01) are also overrepresented among the top downregulated transcripts.

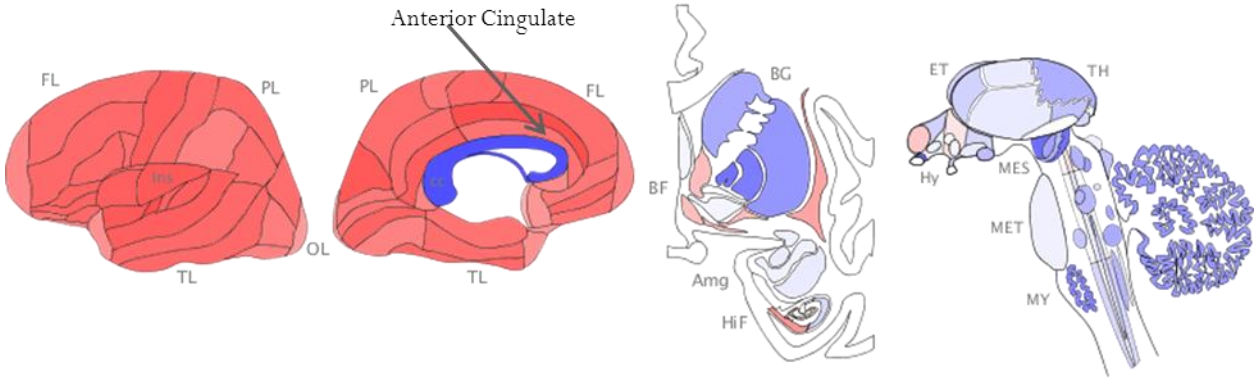

Figure S6: HBAset gene set enrichment of the ten candidate genes considered as a group. The brain regions considered are shown schematically (right to left) for the lateral and medial surfaces of the cortex; basal ganglia and deep temporal lobe; and midbrain, hindbrain and cerebellum at left. Red indicates enrichment, blue indicates “de-enrichment”. Image generated by HBASet.

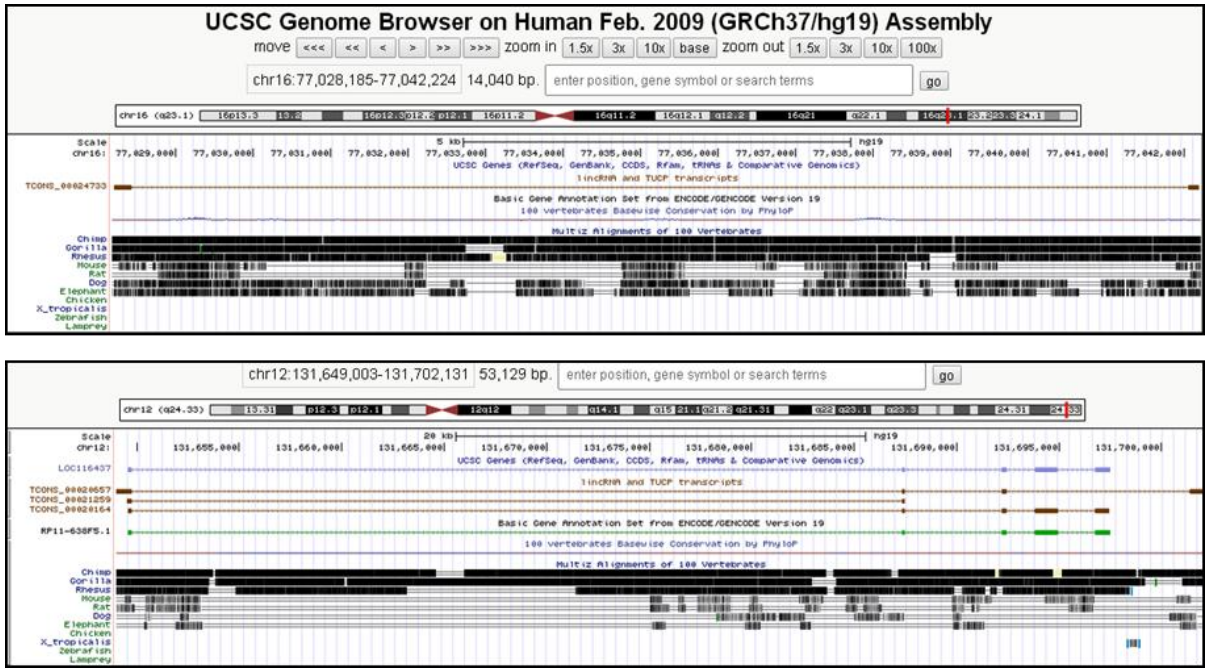

Figure S7: A. Top, Genomic location of linc-KARS-3 (also known as TCONS_0024733). **B. Bottom**, Genomic location of the Chr12 ncRNA locus. linc-SFSWAP-3 (also known as TCONS_0021259) and RP11-638F5.1 (also known as TCONS_0020164) share two exons. Due to the exon-intron distribution at this locus, a qRT-PCR assay (**Figure 3**) specific to linc-SFSWAP-3 could not be designed.

Supplemental References

1. Dumais A, Lesage AD, Alda M, Rouleau G, Dumont M, Chawky N, et al. Risk factors for suicide completion in major depression: a case-control study of impulsive and aggressive behaviors in men. The American journal of psychiatry. 2005;162(11):2116-24.
2. McGirr A, Tousignant M, Routhier D, Pouliot L, Chawky N, Margolese HC, et al. Risk factors for completed suicide in schizophrenia and other chronic psychotic disorders: a case-control study. Schizophrenia research. 2006;84(1):132-43.
3. McGirr A, Paris J, Lesage A, Renaud J, Turecki G. Risk factors for suicide completion in borderline personality disorder: a case-control study of cluster B comorbidity and impulsive aggression. The Journal of clinical psychiatry. 2007;68(5):721-9.
4. Gittins R, Harrison PJ. A quantitative morphometric study of the human anterior cingulate cortex. Brain research. 2004;1013(2):212-22.
5. Vogt BA, Nimchinsky EA, Vogt LJ, Hof PR. Human cingulate cortex: surface features, flat maps, and cytoarchitecture. The Journal of comparative neurology. 1995;359(3):490-506.
6. Hercher C, Parent M, Flores C, Canetti L, Turecki G, Mechawar N. Alcohol dependence-related increase of glial cell density in the anterior cingulate cortex of suicide completers. Journal of psychiatry & neuroscience : JPN. 2009;34(4):281-8.
7. Kim D, Pertea G, Trapnell C, Pimentel H, Kelley R, Salzberg SL. TopHat2: accurate alignment of transcriptomes in the presence of insertions, deletions and gene fusions. Genome biology. 2013;14(4):R36. Epub 2013/04/27.
8. Cabili MN, Trapnell C, Goff L, Koziol M, Tazon-Vega B, Regev A, et al. Integrative annotation of human large intergenic noncoding RNAs reveals global properties and specific subclasses. Genes & development. 2011;25(18):1915-27. Epub 2011/09/06.
9. Anders SP, P.T.; Huber, W. HTSeq – A Python framework to work with high-throughput sequencing data. bioRxiv 2014.
10. Trapnell C, Williams BA, Pertea G, Mortazavi A, Kwan G, van Baren MJ, et al. Transcript assembly and quantification by RNA-Seq reveals unannotated transcripts and isoform switching during cell differentiation. Nature biotechnology. 2010;28(5):511-5.
11. Robinson MD, Oshlack A. A scaling normalization method for differential expression analysis of RNA-seq data. Genome biology. 2010;11(3):R25.
12. Law CW, Chen Y, Shi W, Smyth GK. Voom: precision weights unlock linear model analysis tools for RNA-seq read counts. Genome biology. 2014;15(2):R29.
13. Zhao Z, Xu J, Chen J, Kim S, Reimers M, Bacanu SA, et al. Transcriptome sequencing and genome-wide association analyses reveal lysosomal function and actin cytoskeleton remodeling in schizophrenia and bipolar disorder. Molecular psychiatry. 2014. Epub 2014/08/13.
14. Kim S, Webster MJ. The stanley neuropathology consortium integrative database: a novel, web-based tool for exploring neuropathological markers in psychiatric disorders and the biological processes associated with abnormalities of those markers. Neuropsychopharmacology : official publication of the American College of Neuropsychopharmacology. 2010;35(2):473-82.
15. Dobin A, Davis CA, Schlesinger F, Drenkow J, Zaleski C, Jha S, et al. STAR: ultrafast universal RNA-seq aligner. Bioinformatics. 2013;29(1):15-21.
16. Consortium SM-I. A comprehensive assessment of RNA-seq accuracy, reproducibility and information content by the Sequencing Quality Control Consortium. Nature biotechnology. 2014;32(9):903-14.

17. Liao Y, Smyth GK, Shi W. featureCounts: an efficient general purpose program for assigning sequence reads to genomic features. Bioinformatics. 2014;30(7):923-30. Epub 2013/11/15.
18. Akula N, Barb J, Jiang X, Wendland JR, Choi KH, Sen SK, et al. RNA-sequencing of the brain transcriptome implicates dysregulation of neuroplasticity, circadian rhythms and GTPase binding in bipolar disorder. Molecular psychiatry. 2014.
19. Robin X, Turck N, Hainard A, Tiberti N, Lisacek F, Sanchez JC, et al. pROC: an open-source package for R and S+ to analyze and compare ROC curves. BMC bioinformatics. 2011;12:77. Epub 2011/03/19.
20. Sheridan SD, Theriault KM, Reis SA, Zhou F, Madison JM, Daheron L, et al. Epigenetic characterization of the FMR1 gene and aberrant neurodevelopment in human induced pluripotent stem cell models of fragile X syndrome. PloS one. 2011;6(10):e26203.
21. Andersen CL, Jensen JL, Orntoft TF. Normalization of real-time quantitative reverse transcription-PCR data: a model-based variance estimation approach to identify genes suited for normalization, applied to bladder and colon cancer data sets. Cancer research. 2004;64(15):5245-50.